Journal for Electrochemistry and Plating Technology

JEPT

Edited by: DGO-Fachausschuss Forschung – Hilden / Germany

Electrodeposited Dendrite-Free, Nano-Columnar 3D Lithium Anodes and Their Application in Lithium Sulfur Batteries with 3D Sulfur Cathodes

In this work, homogeneous, dendrite-free, nano-columnar lithium electrodeposition on 3D nickel foam from a 1 M lithium hexafluorophosphate ($LiPF_6$) propylene carbonate (PC) electrolyte under convection has been performed successfully. The surface morphology and the thickness of the deposition can be varied depending on the electrodeposition parameters. In this way, it is possible to improve the surface area and reduce the amount of lithium in the cell, e.g. to only 50 % lithium excess, increasing cell safety. The new lithium plated 3D anode was developed to be combined with a 3D composite electroplated sulfur cathode, ensuring low local current densities at both, cathode and anode, which lowers overpotentials and therefore increase the cell efficiency. Furthermore, the porous electrodes can accommodate a larger amount of...

Received: 2018-05-17
Received in revised form: 2018-05-30
Accepted: 2018-06-06

Keywords: Lithium electrodeposition, lithium sulfur batteries, 3D lithium anode, dendrite-free, nano-columnar

Author: Şeniz Sörgel

DOI: 10.12850/ISSN2196-0267.JEPT6275

LEUZE VERLAG
seit 1902

Electrodeposited Dendrite-Free, Nano-Columnar 3D Lithium Anodes and Their Application in Lithium Sulfur Batteries with 3D Sulfur Cathodes

Şeniz Sörgel

Research Institute for Precious Metals and Metals Chemistry, Katharinenstr. 17, 73525 Schwäbisch Gmünd, Germany

In this work, homogeneous, dendrite-free, nano-columnar lithium electrodeposition on 3D nickel foam from a 1 M lithium hexafluorophosphate ($LiPF_6$) propylene carbonate (PC) electrolyte under convection has been performed successfully. The surface morphology and the thickness of the deposition can be varied depending on the electrodeposition parameters. In this way, it is possible to improve the surface area and reduce the amount of lithium in the cell, e.g. to only 50 % lithium excess, increasing cell safety. The new lithium plated 3D anode was developed to be combined with a 3D composite electroplated sulfur cathode, ensuring low local current densities at both, cathode and anode, which lowers overpotentials and therefore increase the cell efficiency. Furthermore, the porous electrodes can accommodate a larger amount of electrolyte, which is beneficial for an increased cycling stability. The results show that despite the reduction of lithium weight by a factor of 12 compared to a battery with a commercial 1.5 mm thick 2D lithium foil anode, the overall battery capacity on cell level, using cathodes with equal sulfur content, could even be improved.

Keywords: Lithium electrodeposition, lithium sulfur batteries, 3D lithium anode, dendrite-free, nano-columnar **Paper:** Received: 2018-05-17 / Received in revised form: 2018-05-30 / Accepted: 2018-06-06
DOI: 10.12850/ISSN2196-0267.JEPT6275

1 Introduction

Lithium metal is the ultimate choice for a Li battery anode as it has the highest theoretical specific capacity (3860 $mAhg^{-1}$) and lowest electrochemical potential (-3.04 V versus standard hydrogen electrode in aqueous solution) among the battery anode candidates.[1] Due to the latter, maximum cell voltages can be realized with each potential cathode material. In this way, a very high specific energy (proportional to the cell voltage) and specific power (quadratic to the cell voltage) can be achieved. However, commercialization of Li metal containing batteries has not been successful up to now.[2] One of the main obstacles to commercialize metallic Li as a battery anode is the Li dendritic or filiform type growth during charging, which causes short circuits when intergrowing the separator and contacting the cathode. This repeatedly stops the battery from charging, causing safety problems due to heat evolution, dendrite melting and electrolyte destruction. Furthermore, remainings of Li dendrites may inhomogeneously dissolve during discharge, forming isolated ("dead") Li, which leads to an irreversible loss of capacity and causing poor cyclability.[3] After recall of Moli Energy cells with MoS_2 cathode and Li metal anode in the late 80s due to safety con-

cerns[2] and failure to solve the safety problems of the Li metal containing cells in the subsequent years and development of carbonaceous intercalation based anodes by Sony as a successful replacement of Li metal in 90s,[1] Li metal research lost its attraction. Nowadays, however, as Li-ion cells have approached their limits in terms of achievable capacities and the demand for high power and energy density batteries to meet the needs of electronics and automobile applications is increasing enormously, understanding of Li metal chemistry and developing safer and better Li anodes has become a necessity.[4]

Lithium/sulfur (Li/S) cells have received significant research interest in the last years as the theoretical specific battery capacity reaches 1672 $mAhg^{-1}_{sulfur}$ and sulfur is an environmentally friendly material with very low cost.[5-11] There is an enormous Li/S battery research activity in the field of cathode or electrolyte development,[5-11] however, up to date, anode development for Li/S batteries is not much under focus.[6-8,12] So far, commercial, thin Li foils are used at the anode side. However, the 2D Li foils are used much in excess than electrochemically required as very thin Li foils (<50 µm) are commercially not available. The unnecessary Li excess in the battery not only increases the weight of the battery and therefore deteriorates characteristic specific performance parameters of the battery, but also it causes a higher safety risk in case of damage.

Electrodeposition of lithium is an easy and low priced method to produce homogeneous, thin Li layers. Due to its very negative standard reduction potential, lithium cannot be electrodeposited from any aqueous electrolytes as hydrogen would be evolved in favor. This is also reflected by a violent reaction between lithium and water. There are many studies about electrodeposition of Li from aprotic solvents[13-16] or room temperature ionic liquids.[17,18] It is generally known that Li electrodeposition in many electrolyte solutions is highly dendritic.[19] Due to its low melting point and therefore high surface diffusion, the

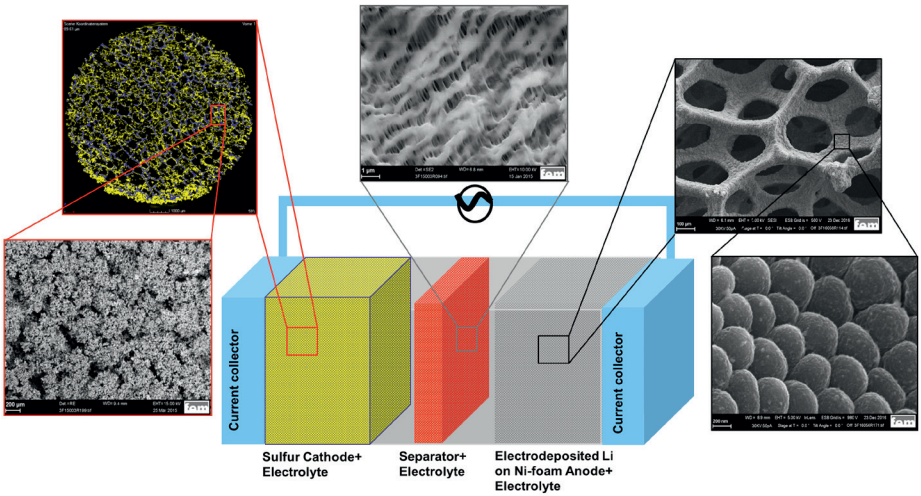

Fig. 1: Schematic view of a Li/S battery with 3D battery electrodes and Celgard 2500 separator

deposition of Li cannot easily be inhibited which turns the deposition diffusion controlled. To prevent dendritic Li growth, several groups suggest the use of HF,[20,21] $CsPF_6$,[22] organic additives,[23] CO_2,[24] H_2O[25] or vinylene carbonate[26] additives. Electrodepositing Li under dynamic conditions ensured by magnetic stirring has also been shown to be successful in terms of dendrite-free Li electrodeposition, as thereby the diffusion limited current is increased[27]. However, up to now, such electrochemically deposited Li anodes have not been tested in Li/S cells.

This paper presents the electrodeposition of homogeneous, non-dendritic, nano-columnar lithium on 3D nickel foam substrates to be used as current collectors in Li/S batteries. The inner porous structure is preserved during electroplating, ensuring a high lithium accessibility in the battery application. In this way, it is aimed to reduce the amount of lithium in the Li/S cell and consequently improve the batteries´ energy density and safety, while the porous structure can keep a larger fraction of electrolyte, improving the batteries´cycling stability. Additionally, with the increased surface area of the anode, it is further a goal to reduce the local current density and overpotential effects to improve the anode kinetics and energy efficiency of the cell. The produced 3D lithium anodes are tested in Swagelok® type cells with 3D sulfur cathodes[28], Celgard 2500 separators and 1 M bis(trifluoromethane)sulfonimide lithium salt (LiTFSI) and 0.75 M lithium nitrate ($LiNO_3$) in (1,2-dimethoxyethane (DME); 1,3-dioxolane (DOL)) (1:1 vol %) electrolyte (*Fig. 1*).

2 Experimental

2.1 Electrodeposition of Lithium

Before Li electroplating, bare 3D nickel foam (RCM-Ni5763.014, Recemat BV, Dodewaard, The Netherlands) (95.2 % foam porosity, 350 µm pore diameter, 1.4 mm foam thickness, 10 mm foam diameter, 7.58 cm^2 surface area) or nickel-foil (Schlenk Metallfolien GmbH, 99.6 %, 32 µm foil thickness, 2 cmx2 cm foil dimensions) were pretreated by cathodic degreasing in SLOTOCLEAN EL KG (Dr.-Ing. Max Schlötter, Geislingen, Germany) with a voltage of 3 V for 20 s and subsequent pickling in 5 vol% H_2SO_4 for 30 s. In this way, the typical oxide layer present on nickel metal was fully removed, ensuring a high adhesion of the deposited layer on the nickel foam or foil substrate. The prepared Ni-substrates were subsequently dried in a vacuum oven at 40 °C and 200 mbar for 24 hours and then immediately transferred into an argon filled glove box.

Cathodic lithium electrodeposition was performed in a glove box under argon atmosphere (99.999 % Ar, $p(O_2)$<0.5 ppm, $p(H_2O)$<0.5 ppm). Lithium foil (Rockwood Lithium GmbH, 135 mm thickness) was used as counter and reference electrode. The electrolyte was 1 M lithium hexafluorophosphate ($LiPF_6$, ≥99.99 %, Sigma-Aldrich) in propylene carbonate (PC, 99.7 %, Sigma-Aldrich). Galvanostatic electrodeposition was performed under magnetic stirring (400 rpm) at current densities of 0.1 mA/cm^2, 0.5 mA/cm^2 and 1 mA/cm^2 by using a MPG2 potentiostat/galvanostat (BioLogic, Grenoble, France) with EC-Lab® software (BioLogic, Grenoble, France).

After electrodeposition, the samples were washed with pure PC to remove residual electrolyte and dried under argon atmosphere at room temperature. The surface morphology of electrodeposited lithium was characterized by a scanning electron microscope (SEM) (Zeiss, Supra 55VP). For the transfer of the electrodeposited Li samples from glove box to the SEM device without air contact, a transfer module (Kammrath&Weiss GmbH) was used.

2.2 Electrochemical Characterization

The electrochemical characterization of the Li electroplated 3D Ni foams was performed at room temperature (25°C-28°C) in a two-electrode Swagelok® type cell with 3D sulfur cathodes.[28] Battery tests were performed in an argon filled glove box (99.999 % Ar, $p(O_2)$<0.5 ppm, $p(H_2O)$<0.5 ppm). Discs with a diameter of 10 mm and 12 mm were used as electrode and separator (Celgard 2500, 25 µm thickness, Celgard, Charlotte, USA), respectively. A solution of 1 M bis(trifluoromethane)sulfonimide lithium salt (LiTFSI, 99.95 %, Sigma-Aldrich) and 0.75 M lithium nitrate ($LiNO_3$, 99.99 %, Alfa-Aesar) in DME:DOL (1:1 vol %) (1,2-dimethoxyethane (DME), 99.5 %, Sigma-Aldrich; 1,3-dioxolane (DOL), 99.8 % Sigma-Aldrich) was used as electrolyte. The electrolyte amount was 105 µL. The total sulfur content of the cathodes was quantified by a combination of total sample oxidation and subsequent SO_2 quantification via a nondispersive infrared sensor (NDIR) (CS 200, Leco Corporation, Saint Joseph, USA). For comparison, commercially available lithium metal (Alfa-Aesar, 99.9 %, thickness 1.5 mm) was used as battery anode while keeping all other parameters same as above.

The charge/discharge performance of the Li/S batteries was investigated by using a MPG2 potentiostat/galvanostat (BioLogic, Grenoble, France) with EC-Lab® software (BioLogic, Grenoble, France). The batteries were cycled, unless otherwise stated, galvanostatically at a current density of 1 $mAcm^{-2}$ (referred to the nominal surface area) between 1.0 V and 3.0 V at room temperature. The cyclic voltammetry (CV) measurements were performed with the same equipment in a three-electrode configuration at a scan rate of 5 mVs^{-1}. As working electrode Ni foil and as counter and reference electrodes Li metal was used. Electrochemical impedance spectroscopy (EIS) was also performed with the same electrochemical workstation. Each spectrum was measured in the frequency range of 500 kHz to 100 mHz and with an excitation voltage of 5 mV. The experimental data were fitted with an equivalent circuit created with Z fit within the EC-Lab® software.

3 Results and Discussion

Surface as well as cross-section SEM images of various electroplated Li on Ni foam substrates show a very homogeneous, strongly structured coating which leads to an increased total surface area (*Fig. 2-9*). Lithium seeds grow in spherical order without any dendrite formation. The cross-section SEM images show that the electrodeposited Li-layer exhibit a nanorod-like structure with spherical column tops (*Fig. 8*). The diameter of the Li columns increase with coating time (*Fig. 8*). The surface morphology and the thickness of the deposition can be varied depending on the electrodeposition parameters. *Fig. 9* shows SEM images with same resolution of electrodeposited Li on Ni foam at different current densities (0.1 $mAcm^{-2}$, 0.5 $mAcm^{-2}$, 1 $mAcm^{-2}$) and coating times (10 min, 1 h, 2 h or 10 h). As current density during electroplating increases, occupation density (number of lithium seeds per nominal area) increases, while preserving a hexagonally dense packed structure. As electrodeposition time increases, the diameter of the spherical Li seeds increases (*Fig. 9*).

Because of the nanostructured surface morphology of the electrodeposited Li, the color of the deposits is not typically gray, but blue-like or red-brown-like instead, depending on the electrodeposition parameters (*Fig. 10*).

The current efficiency during the electrodeposition process was determined as $h=Dm_{deposited}/Dm_{Faraday}$,

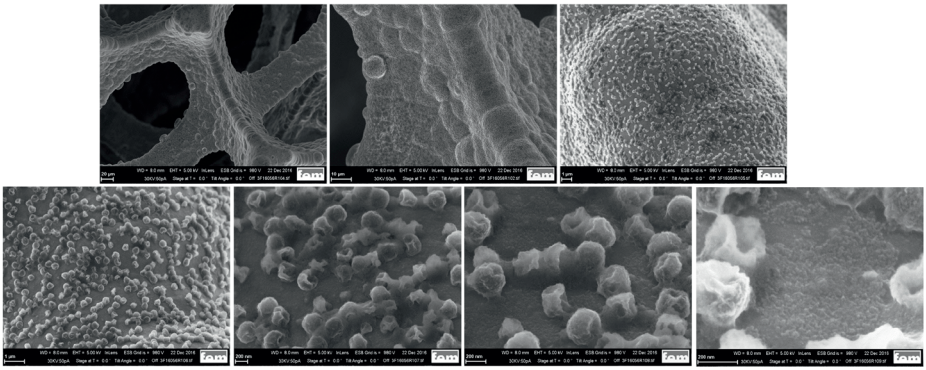

Fig. 2: SEM images of electrodeposited Li on Ni foam at 0.1 mAcm^{-2} for 10 min

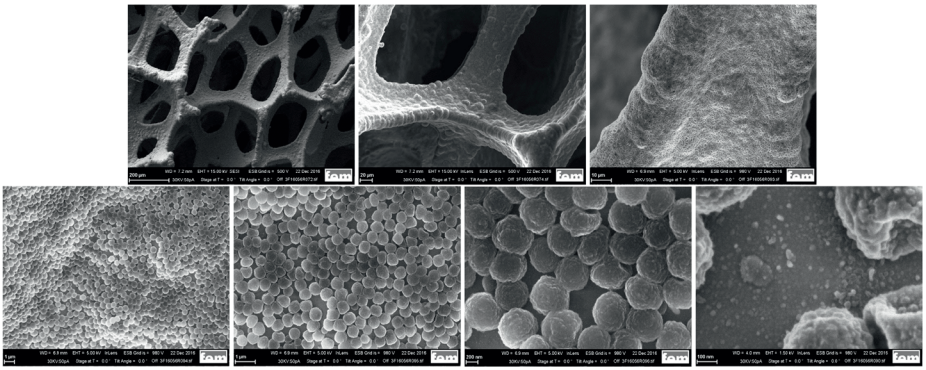

Fig. 3: SEM images of electrodeposited Li on Ni foam at 0.1 mAcm^{-2} for 1 h

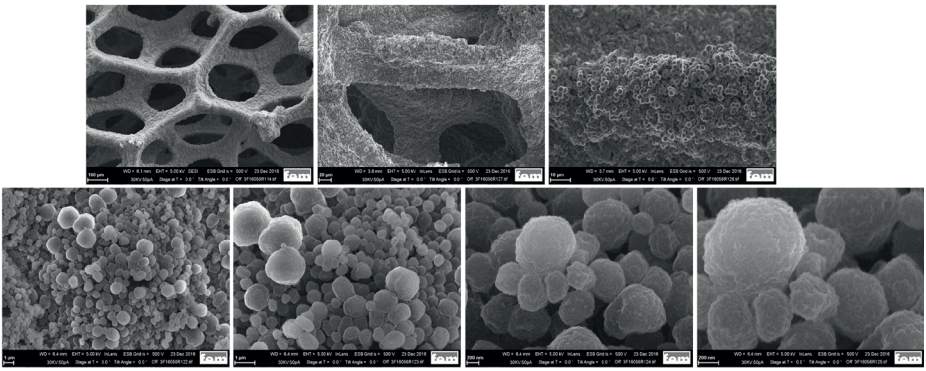

Fig. 4: SEM images of electrodeposited Li on Ni foam at 0.1 mAcm^{-2} for 10 h

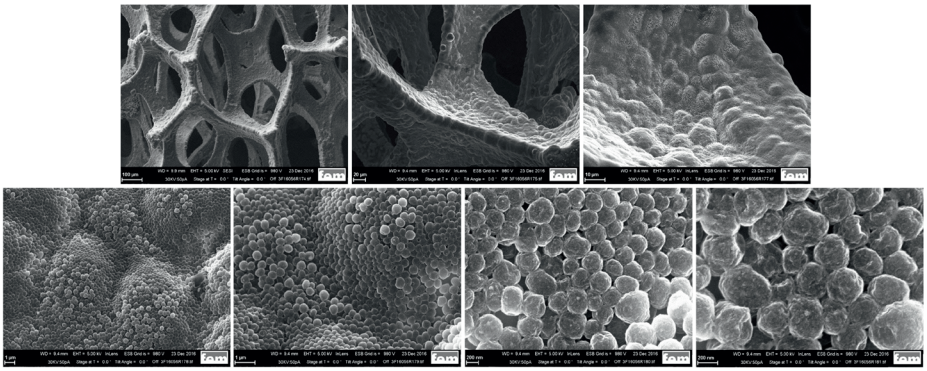

Fig. 5: SEM images of electrodeposited Li on Ni foam at 0.5 $mAcm^{-2}$ for 10 min

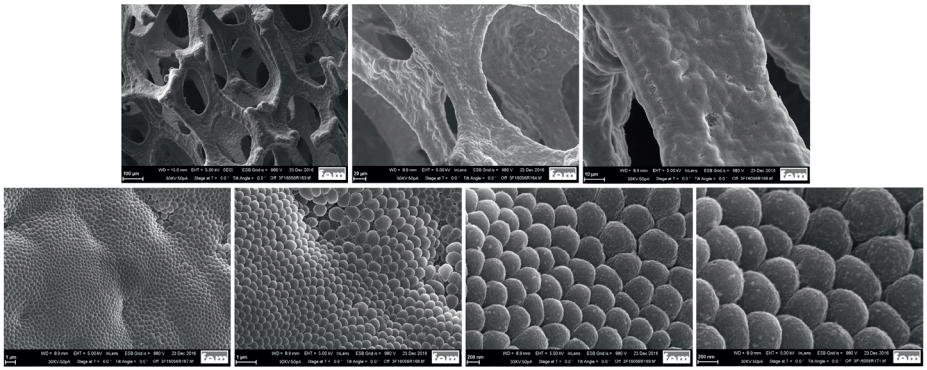

Fig. 6: SEM images of electrodeposited Li on Ni foam at 0.5 $mAcm^{-2}$ for 1 h

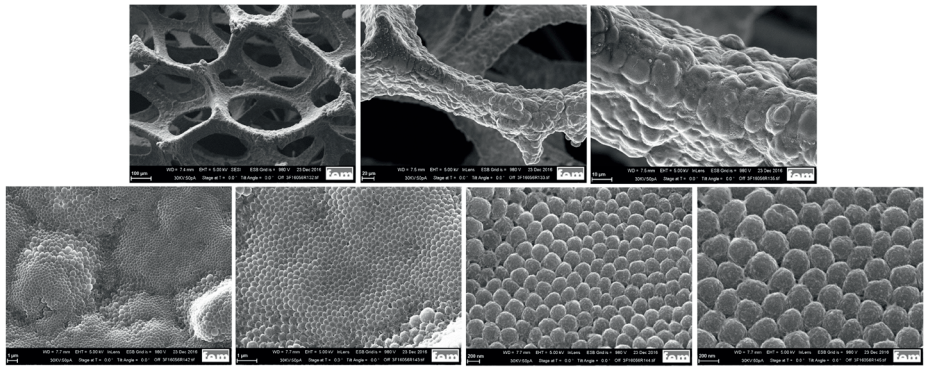

Fig. 7: SEM images of electrodeposited Li on Ni foam at 1 $mAcm^{-2}$ for 10 min

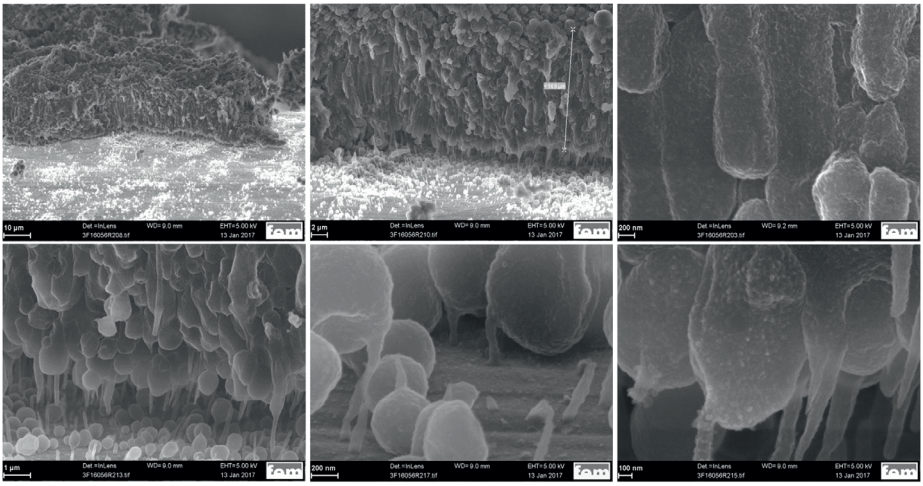

Fig. 8: Cross-section SEM images of electrodeposited Li on Ni foam at 0.1 mAcm^{-2} for 10 h

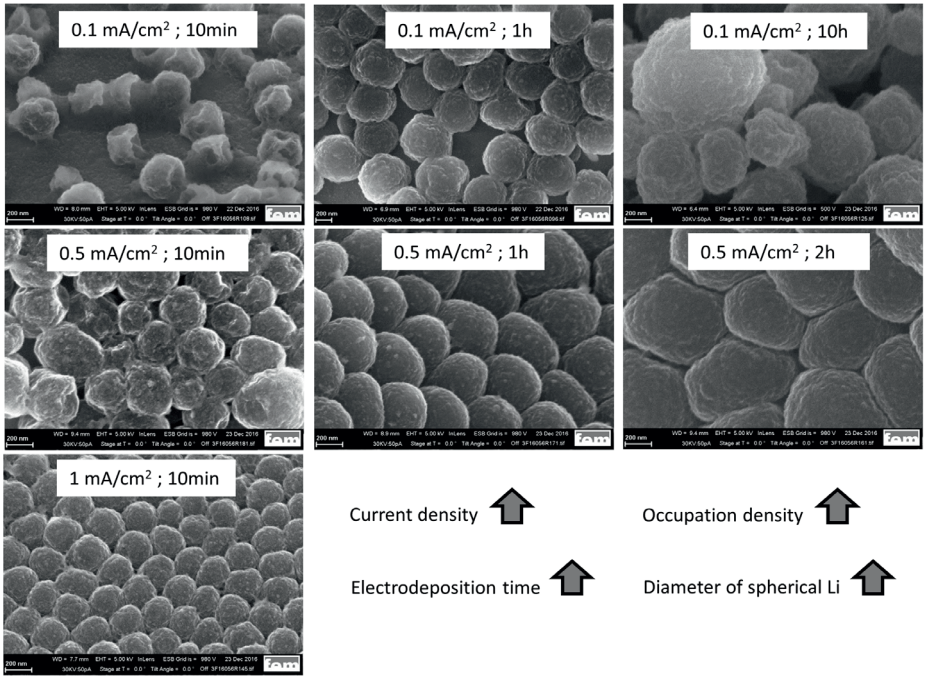

Fig. 9: SEM images of electrodeposited Li on Ni foam at different current densities (0.1 mAcm^{-2}, 0.5 mAcm^{-2}, 1 mAcm^{-2}) and deposition times (10 min, 1 h, 2 h or 10 h)

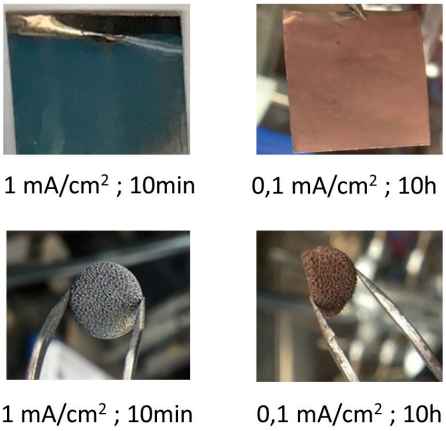

Fig. 10: Optical images of the electrodeposited Li on 2D Ni foil or 3D Ni foam substrates in 1 M $LiPF_6$-PC electrolyte with different electrodeposition parameters

with $Dm_{Faraday}$ being calculated according to the Faraday´s low. As the current efficiency is determined to be 100 %, no significant side-reactions like electrolyte decomposition take place during the electrodeposition process.

The favor of the electrodeposition process is not only to produce non-dendritic lithium layers with a very high specific surface area. It is furthermore possible to apply a tailored and homogeneously distributed amount of lithium and subsequently fine-tune the cell balance by a defined lithium excess. By knowing the current efficiency to be 100 %, this can be done very precisely by applying Faraday´s law.

Figure 11a shows the CV of a Ni electrode in 1 M $LiPF_6$-PC electrolyte. The peaks observed

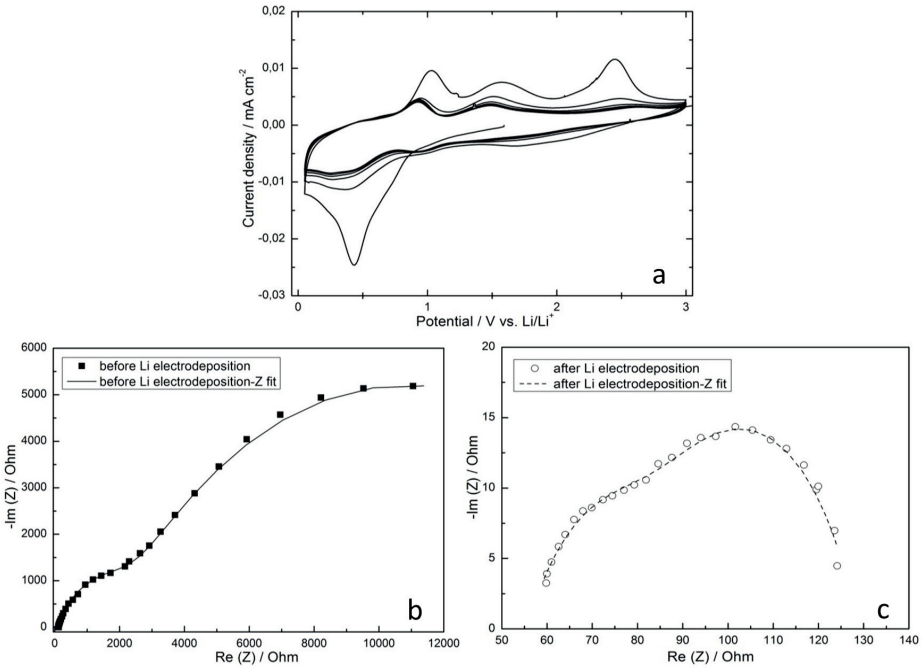

Fig. 11: (a) CV curves for the Ni|Li|Li three-electrode cell in 1 M $LiPF_6$-PC electrolyte. The scan rate was 5 mV s^{-1}, (b, c) EIS spectra of the Ni|Li|Li three-electrode cell in 1 M $LiPF_6$-PC electrolyte before and after Li electrodeposition

during the first cathodic and anodic scans can be assigned to the reductive decomposition reactions of the electrolyte components and the impurities like residual water as well as formation of the SEI layer. The peaks get smaller with increasing cycle number and remain unchanged after the 3th cycle. EIS was further used to investigate the growth of the Li films deposited on a Ni foil substrate (*Fig. 11b and 11c*). The impedance after Li electrodeposition exhibits the typical behavior of a compact thin film (*Fig. 11c*). Two semi-circles are present in each spectrum. The smaller arc in the high-frequency region can be assigned to the impedance of the surface film and the arc in the low-frequency region can be attributed to the charge-transfer reactions.[16]

Figure 12 shows charge-discharge curves of the batteries with Li foil anode (*Fig. 12a*), 3D electrodeposited Li anode (*Fig. 12b*) and the comparison of both anodes at cycles 1, 20, 50 and 70 (*Fig. 12c*). The charge-discharge curves are very similar to the typical Li/S battery curves.[7] The first discharge-curves of both batteries are different from those of the subsequent cycles. The discharging voltages of the 1st cycle are lower and the charging voltages of the 1st cycle are higher than the respective voltages of the subsequent cycles. This is due to the higher overvoltages arising from dissolution of solid sulfur. The first discharge capacity of the battery with Li foil anode and 3D electrodeposited Li anode is 628 mAh g^{-1}_{sulfur} and 305 mAh g^{-1}_{sulfur}, respectively. The lower discharge capacity of the latter might be due to the inac-

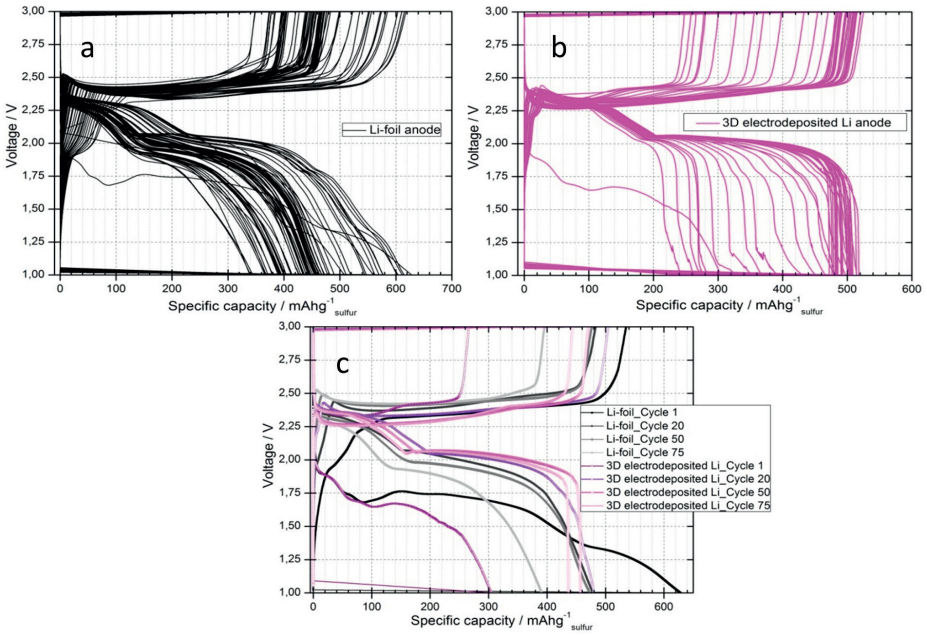

Fig. 12: Charge-discharge curves of the Li/S batteries with 3D sulfur cathodes (6 mg sulfur) and (a) 2D Li foil anode (58.77 mg), (b) 3D electrodeposited Li anode (5 mg Li and 33.5 mg Ni foam) at 1 mA/cm² current density. (c) is the comparison of (a) and (b) at cycles 1, 20, 50 and 75

cessible inner 3D Li surface area by the electrolyte at the beginning of the battery cycling. At cycle 20, a shoulder at 2.33 V and a plateau at 1.99 V are observed during discharging of a battery with Li foil anode. The discharge and charge capacities are 473 mAh g^{-1}_{sulfur} and 477 mAh g^{-1}_{sulfur}, respectively. At the same cycle, a shoulder at 2.36 V and a plateau at 2.03 V are visible with the battery having a 3D electroplated Li anode. The charging and discharging capacities at the 20th cycle are 505 mAh g^{-1}_{sulfur} and 480 mAh g^{-1}_{sulfur}, respectively. Thereby, the capacity values are a little higher than the values of the battery with a 1.5 mm Li foil anode. Increasing battery capacity with 3D electroplated Li anode during the first 20 cycles indicates a concomitant improvement of the sulfur accessibility. With increasing cycle number, the potential of the shoulder and discharge plateau of the battery with Li foil anode decreases. The potentials at cycle 75 are 2.27 V and 1.89 V, respectively. This is an indication of the increased overpotential effects. Additionally, battery capacity decreases with increasing cycle number (charging and discharging capacities at 75th cycle are 396 mAh g^{-1}_{sulfur} and 391 mAh g^{-1}_{sulfur}, respectively). The discharging plateaus of the battery with 3D electroplated Li anode at 75th cycle are at 2.36 V and 2.03 V and thereby remain nearly constant with increasing cycle number. This is an indication of the ignorable overpotential effects with increasing cycle number. The larger electroactive area of the electroplated 3D Li anode can provide a larger Li/electrolyte interface, lower the practical current density and reduce the charge transfer resistance during cycling compared with the planar Li foil. The reduced hysteresis of the 3D electroplated Li anode is in favor of low voltage polarization during discharge/charge in Li/S batteries. The charging and discharging capacities of the battery with electroplated 3D lithium anode at 75th cycle are 444 mAh g^{-1}_{sulfur} and 436 mAh g^{-1}_{sulfur}, respectively.

Nearly identical charging and discharging values of both types of batteries give an indication of ignorable shuttle effects. If there is a pronounced shuttle mechanism in the battery, then the charging capacity significantly exceeds the discharging capacity as unwanted redox reactions take place during charging.

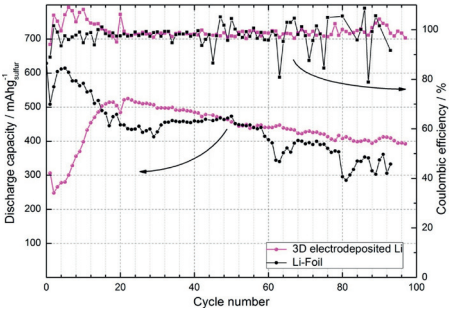

Fig. 13: Cycling stability and coulombic efficiency of the Li/S batteries with 3D sulfur cathodes (6 mg sulfur) and 2D Li foil anode (black curves, 58.77 mg) and 3D electrodeposited Li anode (pink curves, 5 mg Li and 33.5 mg Ni foam) at 1 mAcm^{-2} current density.

In *Fig. 13*, the cyclic performances and coulombic efficiencies of the Li/S batteries with a 2D Li foil anode or with a 3D electrodeposited Li anode are compared. With the 3D electrodeposited Li anode having only 5 mg Li, a specific capacity of about 400 mAhg^{-1} is reached over 100 cycles (*Fig. 13*, pink curve). In comparison, the battery containing 58.77 mg Li foil shows a lower capacity (*Fig. 13, black curve*). The coulombic efficiencies of both batteries are high and stay practically constant at about 98 %.

4 Conclusions

In this work, electrochemical deposition of non-dendritic, nano-columnar lithium layers on 3D Ni foam surface in a 1 M $LiPF_6$-PC electrolyte

under convection has been performed successfully. The surface morphology and the thickness of the deposition can be varied depending on the electrodeposition parameters. As current density during electroplating increases, crystallization rate and therefore occupation density of the Li seeds increases. As electrodeposition time increases, the diameter of the spherical Li seeds increases due to the crystal growth. The current efficiency during Li electrodeposition is found to be 100 %. The favor of the electrodeposition process is not only to produce non-dendritic lithium layers with a very high specific surface area, but also with this method, it is possible to reduce the amount of lithium in the cell and consequently improve the energy density and safety of the cell. The produced 3D Li anodes with only 50 % lithium in excess are tested in Swagelok® type cells with 3D sulfur cathodes.[28] The results show that, although the lithium amount (in weight) at the anode is reduced by a factor of 12 compared to a commercial 2D Li foil, battery capacity remains even better than the battery capacity with a commercial 2D Li foil anode. With the reduced amount of Li in the cell, the Li/S battery safety and energy density can be improved. Additionally, the reduced overpotential effects during discharge/charge of a Li/S battery with a 3D Li anode is a proof of improved anode kinetics and energy efficiency of the cell.

Acknowledgements:

We thank the German Ministry of Economics and Energy for funding this research work under Grad. No. AiF/IGF 19134N. We also thank R. Bretzler and A. Heiß for the SE micrographs.

References:

[1] J. M. Tarascon, M. Armand, Nature, 414, 359 (2001).
[2] K. Brandt, Solid State Ionics, 69, 173 (1994).
[3] D. Aurbach, Solid State Ionics, 148, 405 (2002).
[4] D. Lin, Y. Liu, Y. Cui, Nat. Nanotechnol., 12, 194 (2017).
[5] X. Ji, L. F. Nazar, J. Mater. Chem., 20, 9821 (2010).
[6] Y. X. Yin, S. Xin, Y. G. Guo, L. J. Wan, Angw. Chem. Int. Ed., 52, 13186 (2013).
[7] A. Manthiram, Y. Fu, S. H Chung, C. Zu, Y. S. Su, Chem. Rev., 114, 11751 (2014).
[8] L. Chen, L. L. Shaw, J. Power Sources, 267, 770 (2014).
[9] J. Scheers, S. Fantini, P. Johansson, J. Power Sources, 255, 204 (2014).
[10] D. W. Wang, Q. Zeng, G. Zhou, L. Yin, F. Li, H. M. Cheng, I. R. Gentle, G. Q. M. Lu, J. Mater. Chem. A, 1, 9382 (2013).
[11] S. S. Zhang, J. Power Sources, 231, 153 (2013).
[12] Y. M. Lee, N. S. Choi, J. H. Park, J. K. Park, J. Power Sources, 119-121, 964 (2003).
[13] T. Takei, J. Appl. Electrochem., 9, 587 (1979).
[14] J. Jorné, C. W. Tobias, J. Appl. Electrochem., 5, 279 (1975).
[15] S. Jayakrishnan, M. Pushpavanam, B. A. Shenoi, Surface Technol., 13, 225 (1981).
[16] R. Mogi, M. Inaba, S. K. Jeong, Y. Iriyama, T. Abe, Z. Ogumi, J. Electrochem. Soc., 149, A1578 (2002).
[17] J. Park, J. Lee, C. K. Lee; Appl. Mech. Mater., 217-219, 1049 (2012).
[18] H. Sano, H. Sakaebe, H. Matsumoto, Electrochemistry, 80, 777 (2012).
[19] K. M. Abraham, S. B. Brummer, J. P. Gabano (Ed.), Lithium Batteries, p. 371, Academic Press, London (1963).
[20] S. Shiraishi, K. Kanamura, Z. Takehara, J. Appl. Electrochem., 25, 584 (1995).
[21] K. Kanamura, S. Shiraishi, Z. Takehara, J. Electrochem. Soc., 143, 2187 (1996).
[22] Y. Zhang, J. Qian, W. Xu, S.M. Russell, X. Chen, E. Nasybulin, P. Bhattacharya, M. H. Engelhard, D. Mei, R. Cao, F. Ding, A.V. Cresce, K. Xu, J. G. Zhang, Nano Lett., 14, 6889 (2014).
[23] K. Kanamura, H. Tamura, S. Shiraishi, Z. Takehara, J. Electroanal. Chem., 394, 49 (1995).
[24] T. Osaka, T. Momma, Y. Matsumoto, Y. Uchida, J. Electrochem. Soc., 144, 1709 (1997).
[25] J. Qian, W. Xu, P. Bhattacharya, M. Engelhard, W.A. Henderson, Y. Zhang, J. G. Zhang, Nano Energy, 15, 135 (2015).
[26] H. Ota, K. Shima, M. Ue, J. I. Yamaki, Electrochim. Acta, 49, 565 (2004).
[27] X. Yang, Z. Wen, X. Zhu, S. Huang, Solid State Ionics, 176, 1051 (2005).
[28] Ş. Sörgel, O. Kesten, A. Wengel, T. Sörgel, Energy Storage Materials, 10, 223 (2018).

Author

Şeniz Sörgel
Research Institute for Precious Metals and Metals Chemistry,
Katharinenstr. 17,
73525 Schwäbisch Gmünd,
Germany
Tel.: +49(0)7171 1006-317;
Fax: +49(0)7171 1006-900
E-mail: soergel@fem-online.de

CONTACT:

EUGEN G. LEUZE VERLAG KG
Ralf Schattmaier
Karlstraße 4
88348 Bad Saulgau
Germany

Email: ralf.schattmaier@leuze-verlag.de
Phone: +49 0 7581 4801-12
Fax: +49 0 7581 4801-10